

Nanowired three-dimensional cardiac patches

Tal Dvir^{1,2†}, Brian P. Timko^{1,2†}, Mark D. Brigham³, Shreesh R. Naik¹, Sandeep S. Karajanagi^{1,4}, Oren Levy^{5,6}, Hongwei Jin³, Kevin K. Parker³, Robert Langer¹ and Daniel S. Kohane^{2*}

Engineered cardiac patches for treating damaged heart tissues after a heart attack are normally produced by seeding heart cells within three-dimensional porous biomaterial scaffolds^{1–3}. These biomaterials, which are usually made of either biological polymers such as alginate⁴ or synthetic polymers such as poly(lactic acid) (PLA)⁵, help cells organize into functioning tissues, but poor conductivity of these materials limits the ability of the patch to contract strongly as a unit⁶. Here, we show that incorporating gold nanowires within alginate scaffolds can bridge the electrically resistant pore walls of alginate and improve electrical communication between adjacent cardiac cells. Tissues grown on these composite matrices were thicker and better aligned than those grown on pristine alginate and when electrically stimulated, the cells in these tissues contracted synchronously. Furthermore, higher levels of the proteins involved in muscle contraction and electrical coupling are detected in the composite matrices. It is expected that the integration of conducting nanowires within three-dimensional scaffolds may improve the therapeutic value of current cardiac patches.

The urgent need to improve the viability, ultrastructural morphology and functionality of engineered cardiac tissue has been addressed by developing bioreactors that can provide enhanced mass transfer^{4,7} or expose tissues to electrical⁸ and mechanical cues^{9,10}. The structural and mechanical properties of scaffolds have been improved by microfabrication processes that control stiffness and anisotropy¹¹. Nanostructures incorporated into matrices foster tissue morphogenesis and functionality, improve mechanical and adhesive properties, and direct cells to self-assemble in three dimensions^{12–15}.

The key limitation of porous matrices used for cardiac tissue engineering addressed here is that their pore walls limit cell–cell interaction and delay electrical signal propagation⁶. We have developed three-dimensional nanocomposites of gold nanowires within macroporous alginate scaffolds to bridge the non-conducting pore walls, increase electrical signal propagation throughout the cell-seeded scaffold, and enhance the organization of functioning tissue (Fig. 1). Inorganic nanostructures interact with cardiomyocytes and neurons, for example, to create electronic interfaces^{16–18} and enhance cellular excitability^{19,20}. Gold nanoparticles are promising candidates for tissue engineering because they can be designed to minimize toxicity²¹ and have been used in drug delivery, imaging and cancer therapy²². Such a nanocomposite cellular construct could subsequently be sutured on the infarcted heart to restore function². In time the scaffold will degrade, leaving nanowires embedded within the engineered tissue.

Alginate was selected as a model scaffold material because it has been used extensively in myocardial regeneration^{1,2,23–25}, and has been approved for phase II clinical trials for treating myocardial infarction (MI)²⁶. Like other common scaffolds (collagen, poly(lactico-glycolic acid) (PLGA) and poly(glycerol-sebacate) (PGS)), alginate scaffolds exhibit defined porous structures and favourable biocompatibility, but lack electrical conductivity.

Nanowires should be longer than the average thickness of the alginate pore wall (~500 nm) to interact with cells on both sides, and to enhance electrical signal transmission throughout the scaffold. Nanowires synthesized by anisotropic gold seed elongation^{27,28} had average lengths of 1 μm , diameters of 30 nm (Fig. 2a,b; Supplementary Fig. S1) and zeta potentials of $+45 \pm 3$ mV because of the hexadecyltrimethylammonium bromide (CTAB) capping agent.

A nanocomposite scaffold of alginate and nanowires (Alg–NW) was created by mixing nanowires with sodium alginate, then cross-linking with calcium ions and lyophilizing (Supplementary Fig. S2). The rheology of the alginate gel before lyophilization showed

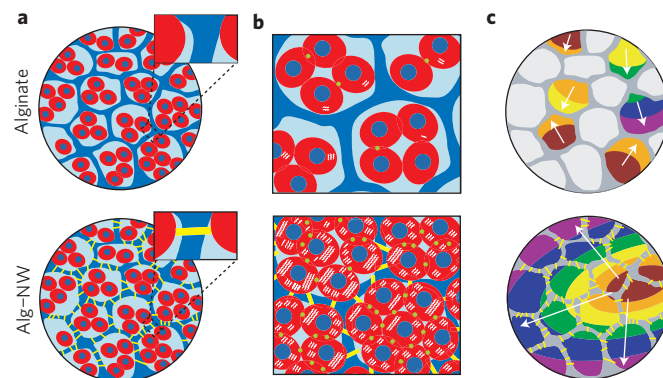


Figure 1 | Schematic overview of three-dimensional nanowire cardiac tissue. a, Isolated cardiomyocytes are cultured in either pristine alginate or Alg–NW composites. Insets highlight the components of the engineered tissue: cardiac cells (red), alginate pore walls (blue) and gold nanowires (yellow). **b**, Whereas cardiomyocytes in pristine alginate scaffolds (top) typically form only small clusters that beat asynchronously and with random polarization, Alg–NW scaffolds (bottom) can exhibit synchronization across scaffold walls, throughout the entire scaffold. **c**, Cardiomyocytes cultured in alginate scaffolds (top) form small beating clusters, but synchronously beating cardiomyocytes in Alg–NW composites (bottom) have the potential to form organized cardiac-like tissue. Colours, contour lines and arrows represent the spatial and temporal evolution of the signal maximum.

¹Department of Chemical Engineering, Massachusetts Institute of Technology, Cambridge, Massachusetts 02139, USA, ²Laboratory for Biomaterials and Drug Delivery, Department of Anesthesiology, Division of Critical Care Medicine, Children's Hospital Boston, Harvard Medical School, 300 Longwood Avenue, Boston, Massachusetts 02115, USA, ³Disease Biophysics Group, Wyss Institute for Biologically-Inspired Engineering, School of Engineering and Applied Sciences, Harvard University, Cambridge, Massachusetts 02138, USA, ⁴Department of Surgery, Massachusetts General Hospital, Harvard Medical School, Boston, Massachusetts 02114, USA, ⁵Harvard-Massachusetts Institute of Technology Division of Health Sciences and Technology, Cambridge, Massachusetts 02139, USA, ⁶Department of Medicine, Brigham and Women's Hospital, Harvard Medical School, Cambridge, Massachusetts 02139, USA.

[†]These authors contributed equally to this work. *e-mail: Daniel.Kohane@childrens.harvard.edu

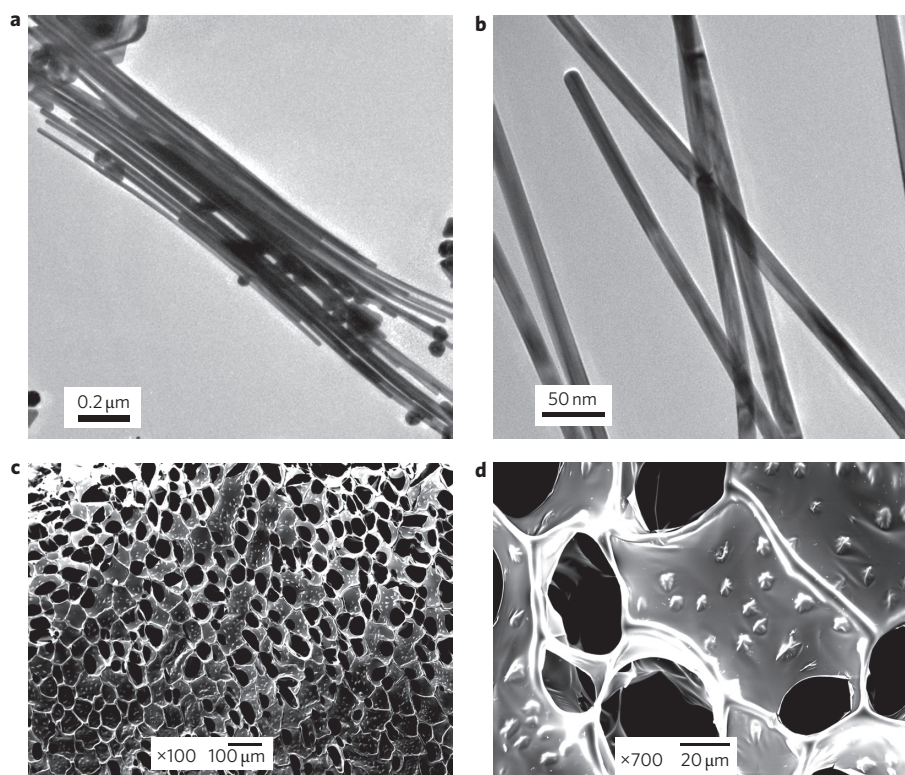


Figure 2 | Incorporation of nanowires within alginate scaffolds. **a,b**, Transmission electron microscopy images of a typical distribution of gold nanowires, which exhibited an average length of $\sim 1 \mu\text{m}$ and average diameter of 30 nm. **c,d**, SEM revealed that the nanowires (1 mg ml^{-1}) assembled within the pore walls of the scaffold into star-shaped structures with a total length scale of $5 \mu\text{m}$. The assembled wires were distributed homogeneously within the matrix (**c**) at a distance of $\sim 5 \mu\text{m}$ from one another (**d**).

increased dynamic viscosity and elastic shear modulus as nanowire concentration was increased (Supplementary Fig. S3). The nanocomposites exhibited improved mechanical properties because the nanomaterials, which interact with the polymers²⁹, act as reinforcements^{30,31}. Here, the positively charged gold nanowires may have interacted electrostatically with the alginate.

The compressive modulus E_c of the wet scaffolds was measured to evaluate their ability to accommodate compressive strain from cardiac beating. The E_c values for alginate and Alg-NW nanocomposites were 1.2 ± 0.2 and $3.5 \pm 0.2 \text{ kPa}$, respectively ($P = 0.008$), which is significantly lower than that of the native heart ($E_c = 425 \pm 9 \text{ kPa}$, $P < 0.001$). Because similar E_c values have been measured for decellularized cardiac matrices³², it is unlikely that Alg-NW scaffolds will inhibit contraction in the engineered tissue. Moreover, scaffolds with lower E_c values have been shown to support cardiac cells and promote the organized contraction of cardiac tissues^{2,10}. As the scaffold degrades and the extracellular matrix is produced, the microenvironment will eventually resemble that of native tissue.

Scanning electron microscopy (SEM) of the scaffolds revealed that at a concentration of 0.5 mg ml^{-1} , nanowires were either parallel to or penetrated the pore walls (Supplementary Fig. S4a). At 1 mg ml^{-1} , the wires formed star-shaped aggregates inside the walls that had dimensions on the scale of $5 \mu\text{m}$ (Fig. 2c,d). Elemental analysis confirmed they contained gold (Supplementary Fig. S4b). At these concentrations, the nanowires were homogeneously distributed $\sim 5\text{--}10 \mu\text{m}$ apart throughout the scaffold.

To simulate the pore wall of the Alg-NW scaffold and to evaluate the bridging effect of the nanowires on the spatial conductivity of the alginate surfaces, we coated $\sim 500\text{-nm}$ -thick films of Alg-NW on indium tin oxide (ITO) conducting glass slides and measured the surface topography and film conductance using conductive

atomic force microscopy (C-AFM; Fig. 3a–d). The many coincident features in the topography and conductance plots indicated that nanowires fully bridged the film. Because the length of the nanowires was not monodisperse and their orientation was random within the films, topographic and conductive coincidences were not identical. At the nanowires, the current was proportional to voltage bias over the range -1 to 1 V , but negligible current passed through nanowire-free regions of the film (Fig. 3e). Higher concentrations of nanowires (2 mg ml^{-1}) increased the conductive coincident features (Supplementary Fig. S5a,b). Alginate films containing gold nanorods significantly shorter than the film thickness (average length, $\sim 60 \text{ nm}$; Supplementary Fig. S6a) showed topographic features similar to those containing nanowires, but negligible electrical current was detected (Supplementary Fig. S6b–d).

Further evidence of enhanced conductivity from nanowires was obtained by measuring the overall film impedance. Films were pressed between two ITO electrodes and an a.c. bias was swept between 1 MHz and 1 Hz (Fig. 3f). All films exhibited relatively low impedance at high frequencies ($>10 \text{ kHz}$) due to capacitive currents through the film. At lower frequencies that encompass the frequency spectrum of mammalian heart rates (on the order of 1 Hz), Alg-NW impedance was consistently lower than in pristine films, a finding attributable to resistive currents through the bridging nanowires becoming increasingly dominant as capacitive currents drop off³³.

We isolated cardiac cells (cardiomyocytes and fibroblasts) from the left ventricles of neonatal rat hearts and seeded them into Alg-NW or pristine alginate scaffolds (see Supplementary Methods). The effect of nanowires on the organization of cardiac cells was studied after culture for three days under static conditions (without electrical stimulation), and again after five days of cultivation under electrical field stimulation to improve cell alignment⁸.

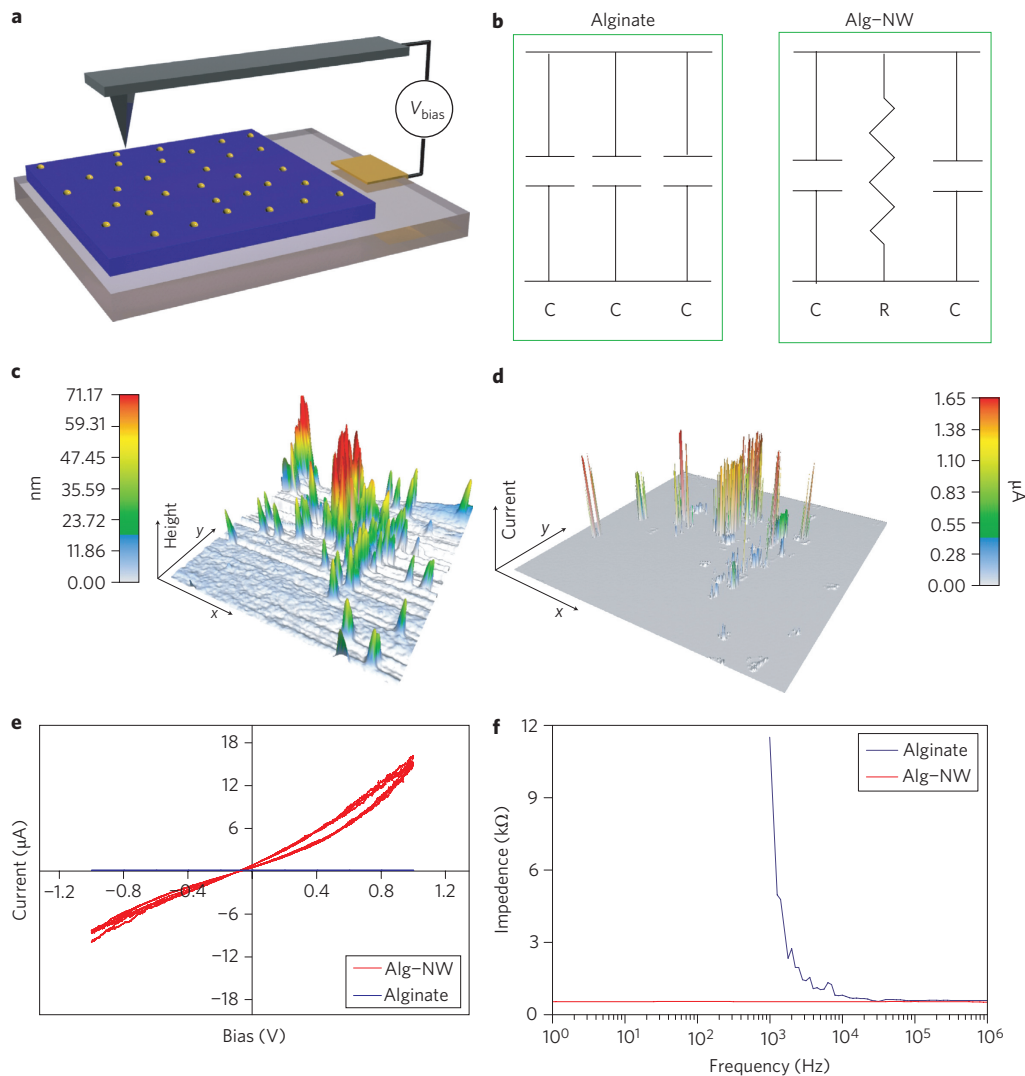


Figure 3 | Increased electrical conductivity of alginate by incorporation of nanowires. **a**, Spatial conductivity was measured by conductive probe atomic force microscopy (C-AFM). The ITO slide served as a backside contact, and the conductive AFM probe was used to simultaneously measure surface topography and conductance through the film. **b**, The equivalent circuit can be represented by capacitors (alginate) and resistors (nanowires) connected in parallel. **c**, Topographic mapping revealed nanowires protruding from the composite alginate thin film ($5 \times 5 \mu\text{m}$). **d**, Spatial conductivity within the Alg-NW film as measured by C-AFM. Current spikes were measured at the location of the nanowires. **e**, Current measured at the nanowires (red) increased with bias voltage over the range -1 to 1 V, while negligible current passed through nanowire-free regions of the alginate film (blue) over the same range. **f**, Overall impedance of the scaffold biomaterial before and after modification with nanowires. Thin layers of Alg-NW or pure alginate films were pressed between two ITO glass slides. These slides served as electrodes and were used to apply an a.c. bias with frequency swept between 1 MHz and 10 Hz. At frequencies near d.c., the impedance of the composite membrane was much lower than that of the pure film.

Typically, cardiac cells seeded in pristine alginate scaffolds do not bind to the matrix, but organize into tight, rounded aggregates ($<200 \mu\text{m}$) within the pores¹⁰. Haematoxylin and eosin (H&E) staining at day 8 revealed thick, intact and better-aligned tissues within the Alg-NW scaffolds (Fig. 4a,b) compared to the small aggregates within alginate scaffolds (Fig. 4c,d). On day 8, nanowires were seen in pore walls (Fig. 4e), suggesting that nanowires remained integrated throughout the cultivation period. H&E-stained thin sections of scaffolds seeded with fewer cells revealed wires in the scaffold walls in close proximity to cell bundles in adjacent pores (Fig. 4f). Based on a metabolic activity assay, neither the nanowires nor their residual chemicals had any cytotoxic effects on the cardiac cells (Supplementary Fig. S7). *In vivo* studies will be crucial for a definitive demonstration of biocompatibility.

The phenotype of the engineered tissue was evaluated by immunostaining for troponin I, which is involved in muscle calcium

binding and contraction, and for the gap junction protein connexin 43 (Cx-43), which is responsible for electrical and mechanical coupling¹⁰. On day 3 (before stimulation), cardiomyocytes within the Alg-NW scaffold expressed higher levels of both proteins (Supplementary Fig. S8a,b). Immunostaining on day 8 revealed strong troponin I fluorescence and cells located throughout the Alg-NW scaffolds (Fig. 4g), but not in the pristine scaffolds (Fig. 4h). In the Alg-NW cultures, Cx-43 between adjacent cardiomyocytes suggested maturation of the tissue (Fig. 4i); this was not seen with unmodified matrices. Western blotting revealed that the Alg-NW cultures had significantly higher amounts of Cx-43 and α -sarcomeric actinin (a protein related to contractile function¹⁰) at days 3 and 8 (Fig. 4j,k and Supplementary Fig. S8c). This means the nanowires imparted phenotypic traits consistent with enhanced electrical and mechanical coupling and contractile properties. The higher Cx-43 level in the Alg-NW scaffold on day 3, before electrical

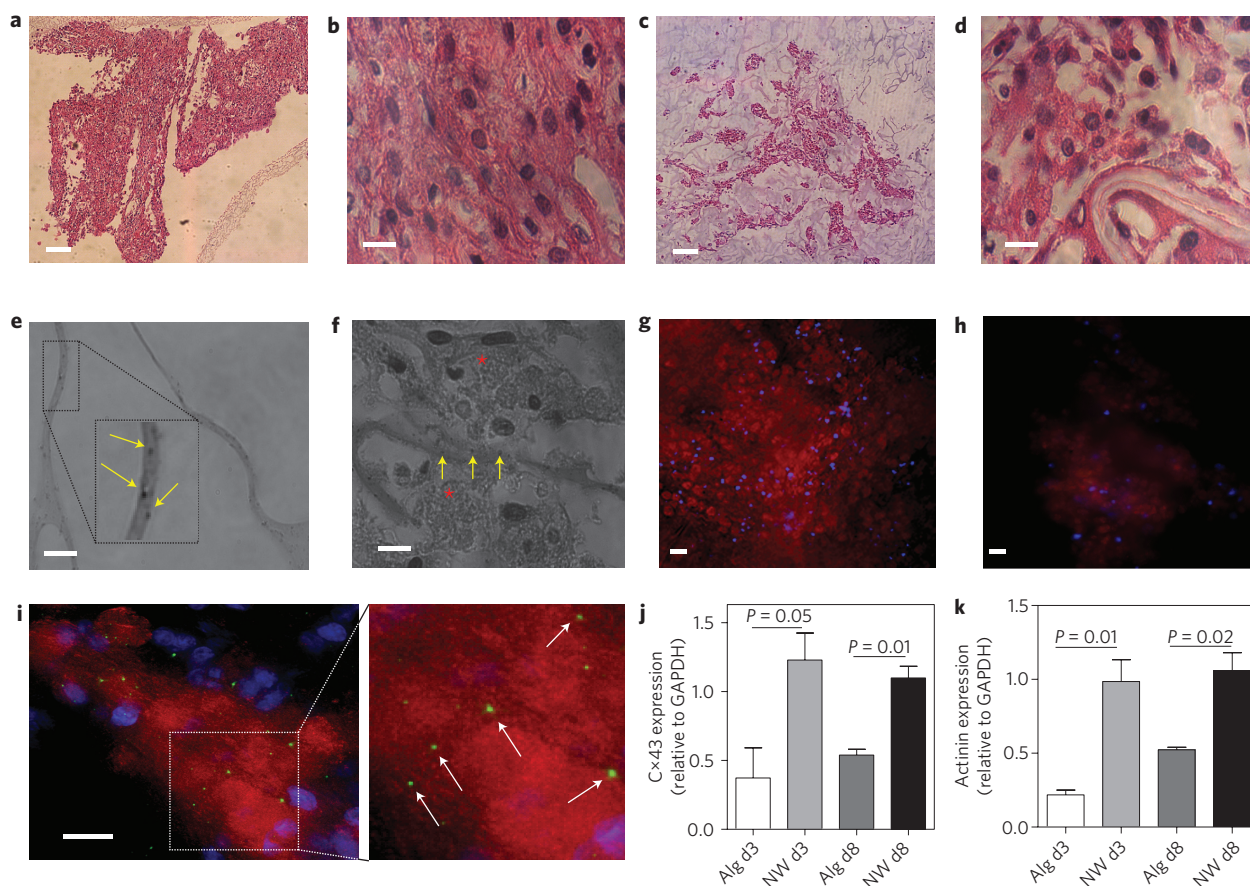


Figure 4 | Cardiac cell organization within the three-dimensional scaffold. **a–d**, H&E stained thin sections of the engineered tissues on day 8 revealed a thick tissue in the nanowire scaffold (**a,b**), whereas the engineered tissue in the pristine scaffolds demonstrated non-continuous tissue separated by pore walls (**c,d**). **e**, Nanowires are seen within the pore walls of a relatively empty region of a scaffold (black dots indicated by yellow arrows). **f**, In a sparsely populated region, wires within the wall (black dots indicated by yellow arrows) were in close proximity to cell aggregates (red asterisks). **g,h**, Immunostaining of the cell-seeded scaffolds on day 8 revealed pervasive troponin I expression (red) within the Alg–NW scaffold (**g**), but less staining was observed in the aggregates in the unmodified scaffolds (**h**). **i**, Connexin 43 gap junction protein was found between cardiomyocytes in the nanowire-containing scaffolds (green dots indicated by white arrows). Nuclei are coloured in blue. **j**, Quantification of connexin 43 protein expression by western blot. **k**, Quantification of sarcomeric actinin protein expression by western blot. Scale bars, 200 μm (**a,c**) or 20 μm (**b,d,e–i**).

stimulation, suggests that the wires affect physiology independently of possible complementary effects of the external electrical field.

Assessment of the electrophysiological effects of nanowires was performed in cardiac cell constructs, with or without nanowires, incubated with a calcium-sensitive dye. Isolated cardiac cell aggregates from each group were stimulated with a local electrical field using microelectrodes. The propagation and green fluorescence intensity of the dye in the engineered tissue were recorded videographically and plotted (Fig. 5). Similar behaviour was observed for six separate constructs in each group. Calcium imaging within pristine scaffolds revealed activity only at the stimulation site, with negligible signal propagation to cells in adjacent pores (Supplementary Movie M1, Fig. 5a,b). Analysis of the recording at six separate sites (Fig. 5a, white circles I–VI) revealed calcium transients only at the stimulus point (I) and not at the nearest other point (II), located slightly more than 100 μm away (Fig. 5b). In contrast, the engineered tissue in the Alg–NW scaffolds contracted synchronously (Supplementary Movie M2, Fig. 5c,d). (Note that the stimulation point was 2 mm to the lower left of point I, that is, far off the lower left corner of the graphic.) In contrast to the lack of signal conduction in the absence of nanowires, recordings at various sites (Fig. 5c, white circles I–V) now revealed calcium transients (Fig. 5d) throughout the scaffold, even though the stimulation point was remote. The calcium transients at sites I–V occurred in a temporal sequence determined

by their spatial relationship to the source of stimulation (Fig. 5e), suggesting continuous propagation of a wavefront of cell depolarization. Furthermore, the calcium transients in the Alg–NW group were significantly higher than in the pristine scaffolds (Fig. 5f).

Many factors may have contributed to the improved scaffold functionality. Nanowires may create conductive bridges across the alginate, connecting adjacent pores and/or cell bundles. Alternatively, the nanowires may directly enhance expression of the electrical coupling protein Cx-43. The improvement in tissue thickness and contractile properties may enhance electrical connectivity and functionality. Because the nanowires were not interconnected structurally (Figs 2, 4e,f) or electrically (Fig. 3, Supplementary Fig. S5), long-range shorting throughout the construct is unlikely. Finally, the effects of nanowires on the viability of fibroblasts, which could also be found in the seeded scaffolds, and the secretion of extracellular matrix by those fibroblasts, may also have affected the functional enhancements observed.

We have demonstrated, for the first time, that nanocomposites of inorganic nanomaterials in polymeric matrices can be used to enhance the structure, phenotype and function of engineered cardiac tissue. Our approach may be useful in creating more homogeneous cardiac patches with stronger contractile properties that could be implanted on the affected surface of a heart after MI. This technique could be generalized to other biomaterials

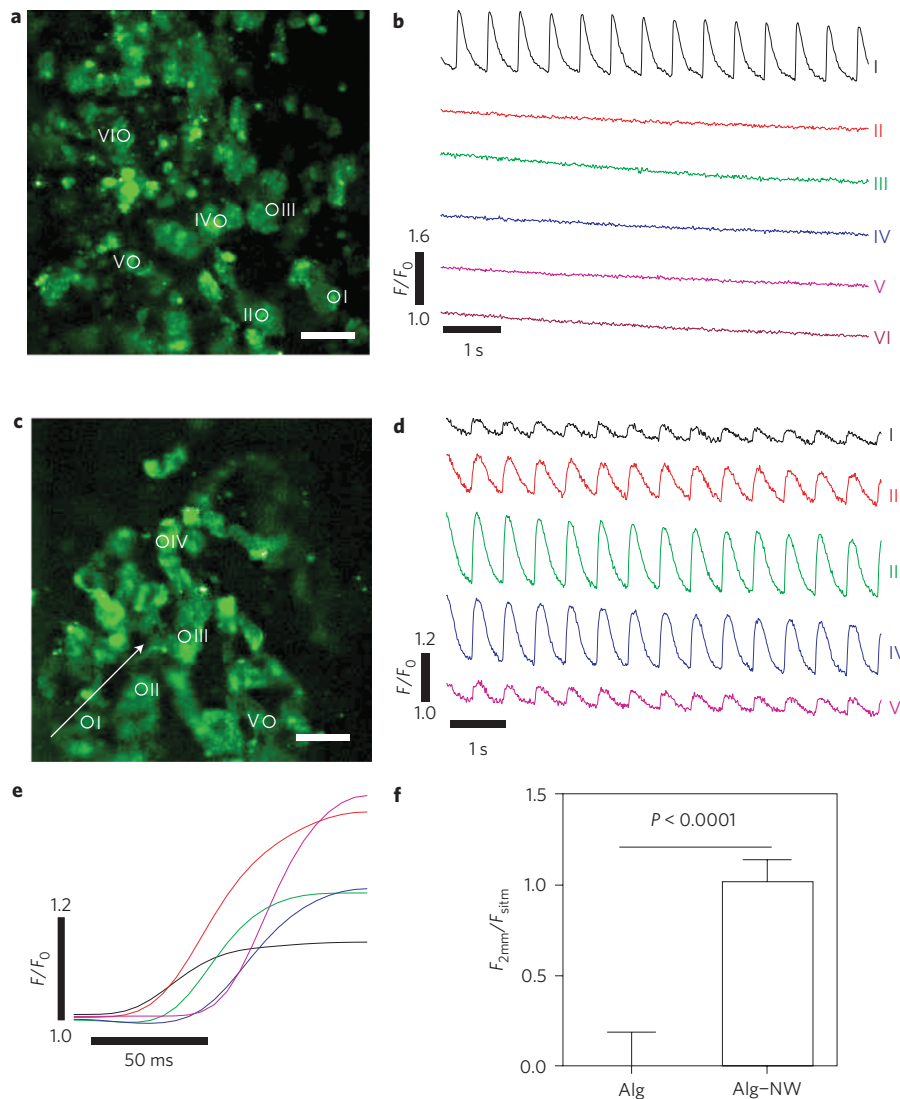


Figure 5 | Calcium transient propagation within engineered tissues. Calcium transient was assessed at specified points (white circles) by monitoring calcium dye fluorescence (green). **a**, Sites monitored in pristine scaffold, where site I is the stimulation point. **b**, Calcium transients were only observed at the stimulation point in the unmodified scaffold. F/F_0 refers to measured fluorescence normalized to background fluorescence. **c**, Sites monitored in an Alg-NW scaffold. The stimulation point was 2 mm diagonally to the lower left of point I (that is, off the figure). The white arrow represents the direction of propagation. **d**, Calcium transients were observed at all points. **e**, Comparison of initial time courses of single signals from sites I–V in **d**. **f**, Quantification of calcium transients (by relative fluorescence) from all samples ($n = 6$ in each group). Bars represent signal maximum transient 2 mm from the stimulation site ($F_{2\text{mm}}$), normalized to the signal maximum at the stimulation site (F_{stim}). Scale bars in **a** and **c**, 100 μm .

such as elastomers or electrospun fibres, and to diseases of other conductive tissues.

Methods

Preparation of gold nanowires. All chemicals were acquired from Sigma-Aldrich and used as received. Nanowires were prepared using an adaption of previously reported methods^{27,28}. First, citrate-capped gold seeds were prepared. A 20 ml aqueous solution of HAuCl_4 (0.25 mM) and sodium citrate (0.25 mM) was prepared. Under vigorous stirring, 0.6 ml ice-cold aqueous NaBH_4 solution (0.1 M) was added at once. The solution immediately turned deep red, consistent with the formation of colloidal gold. A typical product contained spherical gold particles ~ 4 nm in diameter at an estimated density of $\sim 7.6 \times 10^{13}$ particles/ml. The suspension was allowed to stand at room temperature for several hours before use to ensure complete degradation of the NaBH_4 . The gold colloid was stable at 4 °C for at least several months.

Wires were grown by anisotropic elongation of the seeds. To achieve high-aspect-ratio nanowires, the reaction was carried out in three stages, in 25 ml Erlenmeyer flasks (flasks A and B) and a 250 ml round-bottom flask (flask C). First, growth solution was prepared. CTAB (7.54 g, 0.1 M) was dissolved in 200 ml deionized water at 37 °C. After complete dissolution of the CTAB, HAuCl_4 was

added (0.25 mM) followed by ascorbic acid (0.5 mM). The ascorbic acid changed the solution from deep to pale yellow, consistent with the reduction of Au(III) to Au(I) . Finally, HNO_3 (70 mM) was added. The growth solution was then divided between flask A (9 ml), flask B (18 ml) and flask C (173 ml). Nanowire growth was initiated by adding 1 ml seed solution to flask A under vigorous stirring. After 15 s, 1 ml solution was transferred from flask A to flask B, with vigorous stirring. After 30 s, 5 ml solution was transferred from flask B to flask C, with vigorous stirring. The solution in flask C was maintained at 37 °C with stirring, and turned deep purple over the course of 2 h. The solution contained a mixture of morphologies and was subsequently purified. The solution was collected in 50 ml centrifuge tubes, which were then placed in a 37 °C oven and left undisturbed for ~ 1 week. During this time, a brown pellet, which contained $\sim 90\%$ wires, formed at the bottom of each tube. The supernatant was discarded, and the pellets were resuspended in deionized water. A typical synthesis yielded ~ 60 mg product after purification.

Preparation of Alg-NW and alginate scaffolds. The three-dimensional Alg-NW or alginate scaffolds were prepared from pharmaceutical-grade alginate, Protanal LF 5/60 (FMC Biopolymers), which has a high guluronic acid (G) content (65%). The method for Alg-NW scaffold preparation was based on a previously described procedure¹⁰ and is a five-step process, consisting of (1) preparation of sodium alginate stock solutions at concentrations of 1% (w/v); (2) mixing nanowire solution

(1 mg ml⁻¹) with the alginate solution followed by rapid mixing; (3) crosslinking of the alginate/nanowire solution by adding the bivalent crosslinker (for example, calcium gluconate); (4) freezing the crosslinked alginate in a homogeneous, cold (-20 °C) environment; and (5) lyophilization to produce a sponge like scaffold (5 mm × 2 mm, *d* × *h*). The scaffolds were sterilized with ultraviolet light before use and were 90% porous, with pore sizes ranging from 50 to 100 µm in diameter¹⁰. Alginate scaffolds were prepared in the same manner without step (ii).

Intracellular calcium transient measurement. Neonatal rat ventricular myocytes were incubated with 10 µM fluo-4 AM (Invitrogen) and 0.1% Pluronic F-127 for 45 min at 37 °C. Cardiac cell constructs (at least six samples from each group, from three separate experiments) were subsequently washed three times in modified Tyrode solution to allow de-esterification. Cell aggregates were electrically paced at 1–2 Hz using a bipolar platinum electrode placed in close contact with the cells using a micromanipulator. The calcium transients were imaged using a confocal imaging system (LSM 510, Zeiss). The images were acquired with a EC Plan-Neofluar ×10/0.30M 27 objective lens at 216 frame/s 256 × 256 pixels and 2.5 µm/pixel spatial resolution. Fluo 4 was excited with a 488 nm diode laser. Fluorescence (*F*) was normalized by dividing by the basal cell fluorescence (*F*₀) after dye loading. Calcium transient traces were plotted in Igor Pro. For comparison of expanded sections (Fig. 5e), the background noise was reduced using the binomial smoothing algorithm within Igor Pro. For quantification, the intensity maximum of fluorescence was measured using ImageJ software at a point 2 mm from the stimulation spot, for six separate samples in each group.

Statistical analysis. Data are presented as means ± standard deviation (s.d.). Univariate differences between the groups were assessed using Student's *t*-test. All analyses were performed using GraphPad Prism version 5.00 for Windows (GraphPad Software). *P* < 0.05 was considered significant.

Received 20 May 2011; accepted 19 August 2011;
published online 25 September 2011

References

- Leor, J. *et al.* Bioengineered cardiac grafts: a new approach to repair the infarcted myocardium? *Circulation* **102**, III-56–III-61 (2000).
- Dvir, T. *et al.* Prevascularization of cardiac patch on the omentum improves its therapeutic outcome. *Proc. Natl Acad. Sci. USA* **106**, 14990–14995 (2009).
- Zimmermann, W. H. *et al.* Engineered heart tissue grafts improve systolic and diastolic function in infarcted rat hearts. *Nature Med.* **12**, 452–458 (2006).
- Dvir, T., Benishti, N., Shachar, M. & Cohen, S. A novel perfusion bioreactor providing a homogenous milieu for tissue regeneration. *Tissue Eng.* **12**, 2843–2852 (2006).
- Dvir, T., Tsur-Gang, O. & Cohen, S. “Designer” scaffolds for tissue engineering and regeneration. *Israel J. Chem.* **45**, 487–494 (2005).
- Bursac, N., Loo, Y. H., Leong, K. & Tung, L. Novel anisotropic engineered cardiac tissues: studies of electrical propagation. *Biochem. Biophys. Res. Commun.* **361**, 847–853 (2007).
- Radisic, M. *et al.* Medium perfusion enables engineering of compact and contractile cardiac tissue. *Am. J. Physiol. Heart Circ. Physiol.* **286**, H507–H516 (2004).
- Radisic, M. *et al.* Functional assembly of engineered myocardium by electrical stimulation of cardiac myocytes cultured on scaffolds. *Proc. Natl Acad. Sci. USA* **101**, 18129–18134 (2004).
- Zimmermann, W. H. *et al.* Tissue engineering of a differentiated cardiac muscle construct. *Circ. Res.* **90**, 223–230 (2002).
- Dvir, T., Levy, O., Shachar, M., Granot, Y. & Cohen, S. Activation of the ERK1/2 cascade via pulsatile interstitial fluid flow promotes cardiac tissue assembly. *Tissue Eng.* **13**, 2185–2193 (2007).
- Engelmayr, G. C. *et al.* Accordion-like honeycombs for tissue engineering of cardiac anisotropy. *Nature Mater.* **7**, 1003–1010 (2008).
- Dvir, T., Timko, B. P., Kohane, D. S. & Langer, R. Nanotechnological strategies for engineering complex tissues. *Nature Nanotech.* **6**, 13–22 (2011).
- Sachlos, E., Gotor, D. & Czernuszka, J. T. Collagen scaffolds reinforced with biomimetic composite nano-sized carbonate-substituted hydroxyapatite crystals and shaped by rapid prototyping to contain internal microchannels. *Tissue Eng.* **12**, 2479–2487 (2006).
- Souza, G. R. *et al.* Three-dimensional tissue culture based on magnetic cell levitation. *Nature Nanotech.* **5**, 291–296 (2010).
- Wu, S. L. *et al.* A biomimetic hierarchical scaffold: natural growth of nanotitanates on three-dimensional microporous Ti-based metals. *Nano Lett.* **8**, 3803–3808 (2008).
- Timko, B. P. *et al.* Electrical recording from hearts with flexible nanowire device arrays. *Nano Lett.* **9**, 914–918 (2009).
- Timko, B. P., Cohen-Karni, T., Qing, Q., Tian, B. Z. & Lieber, C. M. Design and implementation of functional nanoelectronic interfaces with biomolecules, cells, and tissue using nanowire device arrays. *IEEE Trans. Nanotechnol.* **9**, 269–280 (2010).
- Tian, B. *et al.* Three-dimensional, flexible nanoscale field-effect transistors as localized bioprobes. *Science* **329**, 830–834.
- Lovat, V. *et al.* Carbon nanotube substrates boost neuronal electrical signaling. *Nano Lett.* **5**, 1107–1110 (2005).
- Celot, G. *et al.* Carbon nanotubes might improve neuronal performance by favouring electrical shortcuts. *Nature Nanotech.* **4**, 126–133 (2009).
- Khlebtsov, N. & Dykman, L. Biodistribution and toxicity of engineered gold nanoparticles: a review of *in vitro* and *in vivo* studies. *Chem. Soc. Rev.* **40**, 1647–1671 (2011).
- Giljohann, D. A. *et al.* Gold nanoparticles for biology and medicine. *Angew. Chem. Int. Ed.* **49**, 3280–3294 (2010).
- Hao, X. J. *et al.* Angiogenic effects of sequential release of VEGF-A₁₆₅ and PDGF-BB with alginate hydrogels after myocardial infarction. *Cardiovasc. Res.* **75**, 178–185 (2007).
- Yu, J. *et al.* The effect of injected RGD modified alginate on angiogenesis and left ventricular function in a chronic rat infarct model. *Biomaterials* **30**, 751–756 (2009).
- Ruvinov, E., Leor, J. & Cohen, S. The promotion of myocardial repair by the sequential delivery of IGF-1 and HGF from an injectable alginate biomaterial in a model of acute myocardial infarction. *Biomaterials* **32**, 565–578 (2011).
- ClinicalTrials.gov. ID: NCT01226563. IK-5001 for the Prevention of Remodeling of the Ventricle and Congestive Heart Failure After Acute Myocardial Infarction.
- Gole, A. & Murphy, C. J. Seed-mediated synthesis of gold nanorods: role of the size and nature of the seed. *Chem. Mater.* **16**, 3633–3640 (2004).
- Kim, F., Sohn, K., Wu, J. S. & Huang, J. X. Chemical synthesis of gold nanowires in acidic solutions. *J. Am. Chem. Soc.* **130**, 14442–14443 (2008).
- Mitamura, K., Imae, T., Saito, N. & Takai, O. Fabrication and self-assembly of hydrophobic gold nanorods. *J. Phys. Chem. B* **111**, 8891–8898 (2007).
- Tjong, S. C. Structural and mechanical properties of polymer nanocomposites. *Mater. Sci. Eng. R. Rep.* **53**, 73–197 (2006).
- Balazs, A. C., Emrick, T. & Russell, T. P. Nanoparticle polymer composites: where two small worlds meet. *Science* **314**, 1107–1110 (2006).
- Godier-Furnemont, A. F. *et al.* Composite scaffold provides a cell delivery platform for cardiovascular repair. *Proc. Natl Acad. Sci. USA* **108**, 7974–7979 (2011).
- Horowitz, P. & Hill, W. *The Art of Electronics* (Cambridge Univ. Press, 1989).

Acknowledgements

This research was funded by the National Institutes of Health (NIH, grants GM073626 to D.S.K. and DE13023 and DE016516 to R.L.). T.D. thanks the American Heart Association for a Postdoctoral Fellowship. B.P.T. acknowledges an NIH Ruth L. Kirschstein National Research Service Award (no. F32GM096546). The authors would like to thank H. Park, B. Tian, D. Liu, A. Argun and L. Bellan for their assistance and discussions.

Author contributions

T.D. and B.P.T. conceived the idea. T.D., B.P.T., K.K.P., R.L. and D.S.K. designed the experiments and interpreted the data. T.D., B.P.T., M.D.B., S.R.N., S.S.K. and O.L. performed the experiments. H.J. analysed data. T.D., B.P.T. and D.S.K. co-wrote the paper.

Additional information

The authors declare no competing financial interests. Supplementary information accompanies this paper at www.nature.com/naturenanotechnology. Reprints and permission information is available online at <http://www.nature.com/reprints>. Correspondence and requests for materials should be addressed to D.S.K.